

Position Controller for PMSM Based on Finite Control Set Model Predictive Control

Viktor Slapak¹, Karol Kyslan¹, Frantisek Durovsky¹

¹*Department of Electrical Engineering and Mechatronics, Technical University of Kosice,
Letna 9, 042 00 Kosice, Slovakia
viktor.slapak@tuke.sk*

¹Abstract—The paper presents the position control of a permanent magnet synchronous motor by using the finite control set model predictive control. The position, speed and acceleration references are generated by a ramp generator. A new cost function, including feed-forward and load torque compensations, is introduced. In order to save the computational power, a combination of a predictive speed control with proportional position controller is explored as well. Presented methods are compared to the conventional field oriented control structure by a simulation.

Index Terms—Predictive control; permanent magnet motors; position control.

I. INTRODUCTION

The most of today's industrial productions use robotic lines or robotic tools to increase the production rate and to secure the high precision in product assembling. The base of such industrial tool is often an electrical drive, which has to fulfil various demands. The most important are high dynamics, high precision and very often compact dimensions. Of course, such demands are very common to more sectors than just industry. As an example we can mention motion control applications or medical tools.

The permanent magnet synchronous motor (PMSM) is mostly chosen in such cases due to its undisputed advantages, which fully comply with aforementioned demands. Moreover, PMSM offers high torque vs. weight ratio, relatively easy control comparing to asynchronous motor and simpler construction comparing to DC machine, thus making PMSM more reliable and maintenance cost effective.

The electrical drives with PMSM are mostly controlled by the field-oriented control (FOC) with the position sensor or sensorless using various sensorless control techniques [1], [2]. The research today is focused on improving sensorless control techniques of PMSM with respect to high accuracy of the speed control in slow speed range [3] or high position accuracy in case of position controlled drives [4].

Although PMSM drives with FOC control are considered as high dynamic drives, there are still efforts to improve its dynamics by using direct torque control techniques [5] or by using model predictive control.

Model predictive control (MPC) is based on the prediction of future behaviour of the drive and then choosing the best action to fulfil given requests. In fact, the MPC can use a pulse-width modulation with online or offline computation [6], [7], or so-called finite control set model predictive control (FCS-MPC) based on switching possibilities of the inverter [8]–[10].

The most of FCS MPC research is focused on the current control [11], torque control [12] or current control in combination with other controllers [13] or on the speed control of PMSM [14], [15]. FCS-MPC position control has not been much explored yet. This paper deals with the FCS-MPC based position control of PMSM. A ramp generator is used to generate S-curve position reference. Speed and current references from the generator are used as necessary values for the feed-forward compensations of dynamic current and speed. Moreover, we have introduced actual current control in the way to compensate load torque and friction.

FCS-MPC in general requires high computational power. Its computing demands are higher in dependence of controlled system order. Therefore, we have also explored a combination of FCS-MPS speed control with P type position controller.

At first, the paper describes the mathematical model of PMSM in the Section II. Next, noise filtering by using the Kalman filter is briefly described in the Section III. Section IV is dedicated to the main principle of the FCS-MPC.

II. MATHEMATICAL MODEL OF PMSM

The mathematical model of PMSM, used in proposed control, is described in rotor coordinates according to [16], [17]:

$$\frac{di_d}{dt} = -\frac{R}{L_d}i_d + \frac{L_q p \omega_r}{L_d}i_q - \frac{1}{L_d}u_d, \quad (1)$$

$$\frac{di_q}{dt} = -\frac{R}{L_q}i_q - \frac{L_d p}{L_q}\omega_r i_d - \frac{\lambda p}{L_q}\omega_r - \frac{1}{L_q}u_q, \quad (2)$$

$$T_e = \frac{3p\lambda}{2}i_q = k_t i_q, \quad (3)$$

$$\frac{d\omega_r}{dt} = \frac{k_t}{J}i_q - \frac{B_\omega}{J}\omega_r - T_l, \quad (4)$$

$$\frac{d\phi_r}{dt} = \omega_r, \quad (5)$$

where R is the motor winding resistance, L_d and L_q are the motor winding inductances, p is the number of pole-pairs, k_t is the motor torque constant, λ is the rotor flux linkage, J is the total drive inertia, i_d , i_q and u_d , u_q are the motor current and voltage components, ω_r and ϕ_r are the rotor speed and position, T_l is the load torque, B_ω is the viscous friction coefficient and p is the number of pole pairs.

State-space representation is written in the form:

$$\dot{\mathbf{x}}(t) = f_c(\mathbf{x}(t), \mathbf{u}(t), T_l(t)), \quad (6)$$

$$\mathbf{y}(t) = \mathbf{x}(t), \quad (7)$$

where the f_c is a nonlinear function and the state vector $\mathbf{x}(t)$ and the output vector $\mathbf{y}(t)$ are defined as follows:

$$\mathbf{x}(t) = \begin{bmatrix} i_d \\ i_q \\ \omega_r \\ \phi_r \end{bmatrix}, \quad (8)$$

$$\mathbf{y}(t) = \begin{bmatrix} i_d \\ i_q \\ \omega_r \\ \phi_r \end{bmatrix}. \quad (9)$$

However, for the prediction and noise filtering, a discrete model is needed. It has been obtained by using Taylor series expansion

$$x_j(k+1) = x_j(k) + \sum_{l=1}^{N_j} \frac{T_s^l}{l!} \left. \frac{d^l x_j}{dt^l} \right|_{t_k}, \quad (10)$$

where T_s is the sampling time, N is the order of the last member of the expansion, k is the sampling step and j is the j^{th} state of the system.

Here, a special attention must be taken. If we consider one-step prediction horizon, inputs should explicitly appear in every state, thus enabling direct feed-through from the actuation input to the all states [18]. Therefore, 1st order expansion is needed for the current components, 2nd order in case of speed equation and 3rd order for the position part.

III. NOISE FILTERING AND LOAD TORQUE ESTIMATION

In order to get smoother measurement results, various filters can be used, e.g. 1st order or moving average filters. In this paper, a Kalman filter was used due to its filtering capabilities. The second reason for choosing the Kalman filter is the possibility to estimate a load torque (under assumption of relatively slow changes of the load torque, which is a typical case).

The Kalman filter (KF) is designed in the form of predictor-corrector [19] and it is based on the motor model from Section II. We assume that the current components,

angular speed and position are measured.

The Kalman filter equations are written as:

$$\mathbf{x}_c(k) = \mathbf{x}_p(k) + \mathbf{K}(k) [\mathbf{y}(k) - \mathbf{y}_p(k)], \quad (11)$$

$$\mathbf{x}_p(k+1) = f(\mathbf{x}_c(k), \mathbf{u}(k)), \quad (12)$$

$$\mathbf{y}_p(k) = \mathbf{C}_d \mathbf{x}_p(k). \quad (13)$$

In (10), $\mathbf{K}(k)$ is the Kalman gain matrix, f is the nonlinear function based on (1)–(5), \mathbf{C}_d is the output matrix, $\mathbf{x}_p(k)$ is the vector of the observer states, $\mathbf{y}(k)$ and $\mathbf{y}_p(k)$ are the system and observer outputs, $\mathbf{u}(k)$ is the vector of the system inputs, and $\mathbf{x}_c(k)$ is the vector of corrected (filtered) states used for the prediction.

Here, two approaches are possible. At first, we can filter all system states. However, this leads to a nonlinear version of KF thus needing a lot of computational power. The second possibility is to consider current measurements as a reliable with the minimum noise. Then, we can design KF only for the mechanical part of the drive and therefore, linear KF is satisfactory. This significantly reduces computational power requirements, but the current components remain unfiltered.

In this paper, we used the nonlinear Kalman filter, according to filter equations (11)–(13), thus sacrificing computation time in order to achieve a better state filtering. In that case, the vector of corrected states is defined as follows

$$\mathbf{x}_c = \begin{bmatrix} \hat{i}_d(k) \\ \hat{i}_q(k) \\ \hat{\omega}_r(k) \\ \hat{\theta}_r(k) \\ \hat{T}_l(k) \end{bmatrix}, \quad (14)$$

where $\hat{T}_l(k)$ is the observed load torque. As can be seen from (14), an augmented state-space was used in order to estimate load torque.

IV. PRINCIPLE OF DESIGNED FCS MPC

The main idea behind FCS MPC lies in the fact that the inverter has only limited amount of admissible switching states. For voltage source inverter there are only 8 admissible states (six different non-zero voltage vectors and two possibilities for zero voltage vector) [8].

For each of them, we can predict the future states of the drive and choose the most suitable switching state to fulfil our demands.

A. State Prediction

For the sake of minimizing computational time, one-step prediction horizon is chosen. If more steps were used, computation time would rise significantly. For example, in two-step horizon, 49 predictions are needed instead of 7 predictions in one-step prediction horizon.

The predictors are based on discrete model of PMSM and are defined as follows:

$$\begin{bmatrix} i_{dj}(k+1) \\ i_{qj}(k+1) \\ \omega_{rj}(k+1) \\ \phi_{rj}(k+1) \end{bmatrix} = f(\mathbf{x}_{flt}(k), u_j, \hat{T}_l(k)), \quad (15)$$

$$\mathbf{x}_{flt} = \begin{bmatrix} \hat{i}_d(k) \\ \hat{i}_q(k) \\ \hat{\omega}_r(k) \\ \hat{\theta}_r(k) \end{bmatrix}, \quad (16)$$

where subscript j stands for the computation with j^{th} voltage vector.

B. Cost Function

The analytical expression of our demands on the drive can be written as an optimization problem or a cost function, which is to be minimized. The basic cost function used in the paper is defined as follows

$$G = \underbrace{w_1 (\phi_{ref} - \phi_{rj})^2}_a + \underbrace{w_2 (\omega_{ref} - \omega_{rj})^2}_b + \underbrace{w_3 (i_L + i_{B\omega} + i_{dyn} - i_{qj})^2}_c + \underbrace{w_4 i_{dj}^2}_d + \underbrace{f_{lim}(i_{dj}, i_{qj})}_e. \quad (17)$$

where w_i are the tunable weighting factors, i_{dj} , i_{qj} , ω_{rj} , ϕ_{rj} are the outputs of predictors for j^{th} voltage vector.

It consists from five terms:

- a - this term assures tracking of a position reference ϕ_{ref} ,
- b - this term assures tracking of a speed reference ω_{ref} ,
- c - this term represents a current controller with a feed-forward compensations,
- d - minimizes a flux-creating current to maximize torque-per-ampere ratio,
- e - current limitation.

Current reference in term c is combined from a static load torque component i_L , a friction-compensating current component $i_{B\omega}$ and from a dynamic feed-forward component i_{dyn} :

$$i_L = \frac{\hat{T}_l}{k_t}, \quad (18)$$

$$i_{B\omega} = \frac{B_\omega \hat{\omega}_r}{k_t}, \quad (19)$$

$$i_{dyn} = \frac{J \varepsilon_{ref}}{k_t}, \quad (20)$$

where ε_{ref} is reference angular acceleration available from the ramp generator (see subsection C).

The current limitation works on the simple principle. If predicted current is higher than limit i_{max} , the cost function would have very high value (ideally infinite) for given voltage vector, thus forcing the controller to choose other vector:

$$f_{lim}(i_{dj}, i_{qj}) = \begin{cases} 0 & \text{if } \sqrt{(i_{dj}^2 + i_{qj}^2)} \leq i_{max}, \\ \infty & \text{if } \sqrt{(i_{dj}^2 + i_{qj}^2)} > i_{max}. \end{cases} \quad (21)$$

C. Ramp Generator

Reference signals for PMSM control are taken from a simple ramp generator based on following:

$$\omega_{ref} = \int \varepsilon_{ref} dt, \quad (22)$$

$$\phi_{ref} = \int \omega_{ref} dt, \quad (23)$$

where ε_{ref} is a square wave user defined function.

This generation of the reference position is commonly used in the commercial power converters, especially in the servo control, when smooth positioning is required.

D. Control Structure

Control structure of the FCS-MPC position control is in Fig. 1. As can be seen, all states are directly controlled by MPC controller, therefore prediction of PMSM position is needed. However, position prediction, as is based on (15) with 3rd order expansion requires relatively high amount of the computational power. Moreover, tuning of the weighting factors can be difficult, because when the order of the system becomes higher, the change of the controlled states between two samples is decreasing. Therefore, very high weighting factors for the position control term need to be chosen, in comparison to the other weighting factors.

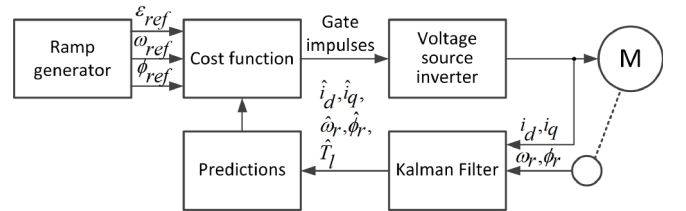


Fig. 1. Block diagram of full FCS-MPC position controller.

In order to obey such a situation, a combination of using P type position controller and FCS-MPC speed control is explored (Fig. 2). In this case, it is expected that the dynamics of the position correction will be a bit lower. On the other hand, computing time savings are further expected.

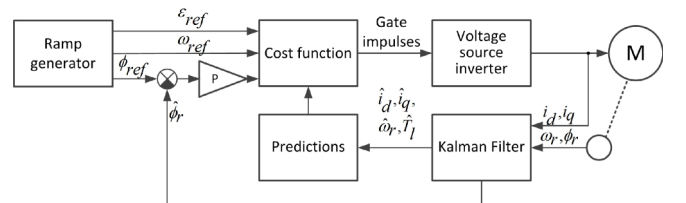


Fig. 2. Block diagram of FCS-MPC position control in combination with proportional position controller.

The weighting factors w_2 , w_3 and w_4 in (17) for FCS-MPC speed controller in combination with P controller are set to the same values, as the weighting factors for fully FCS-MPC based position control.

V. SIMULATION RESULTS

Proposed control structures were simulated with the

sampling time $T_s = 25 \mu\text{s}$ with the mathematical model of 240 W PMSM drive, parameters of which can be found in Appendix A.

For the simulation purposes, working cycle was chosen as in Table I with the weighting factors set as in Table II.

TABLE I. DESCRIPTION OF THE SIMULATION RUN.

Simulation Time	Event
0.05 s–0.01 s	Constant acceleration with $\epsilon_{ref} = 4500 \text{ s}^{-2}$
0.01 s	Steady state with $\omega_r = 200 \text{ s}^{-1}$
0.15	Load torque of $T_l = 0.4 \text{ Nm}$ is applied
0.2 s–0.25 s	Constant deceleration with $\epsilon_{ref} = -4500 \text{ s}^{-2}$
0.25 s	Steady state with $\omega_r = 0 \text{ s}^{-1}$
0.3 s	Load torque is lowered to $T_l = 0.2 \text{ Nm}$

TABLE II. WEIGHTING FACTORS VALUES.

Weighting factor	Value for position FCS-MPC	Value for speed FCS-MPC with proportional position controller
w_1	10^4	-
w_2	$2 \cdot 10^{-4}$	$2 \cdot 10^{-4}$
w_3	$5 \cdot 10^{-6}$	$5 \cdot 10^{-6}$
w_4	$3 \cdot 10^{-6}$	$3 \cdot 10^{-6}$

Note that in the case of the proportional position controller with FCS-MPC speed controller, term a in the cost function (17) and the prediction of the position is not present. The value of the proportional controller is set to the same value as in FOC control structure.

Presented controllers were compared to the conventional cascade FOC structure with PI controllers involving the common compensations. Influence of PWM modulation in FOC is added to the simulation, but simulation runs with the ideal switches, and so dead-band is not considered. During the simulations, all states defined in (8) were observed and compared.

From the comparison of both current components in Fig. 3 and in Fig. 4 it is obvious that the waveform with the lowest oscillations belongs to classical FOC control structure, although there are some undesirable peaks during the transients. The current waveforms of both MPC approaches are very similar. Note that the current oscillations in FOC waveforms occur due to pulse-width modulation with 10 kHz carrying frequency.

Speed reference tracking is depicted in Fig. 5. As can be seen from the detailed view, both MPC controllers have faster dynamics than FOC control structure, thus providing better speed tracking against FOC.

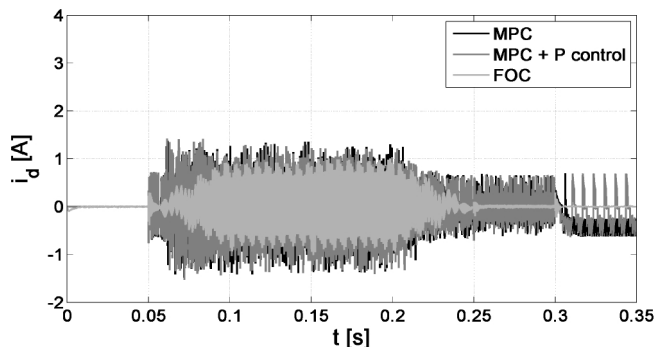


Fig. 3. Simulation comparison of current d-components.

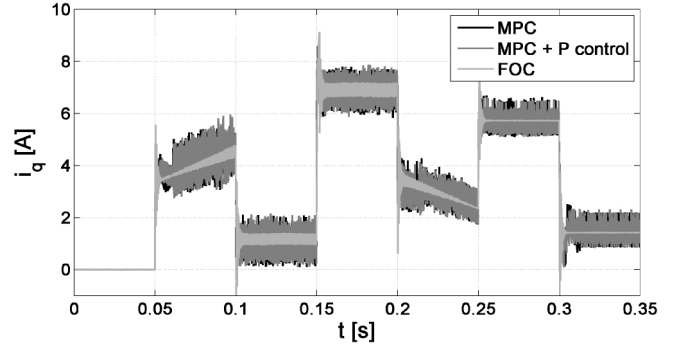


Fig. 4. Simulation comparison of current q-components.

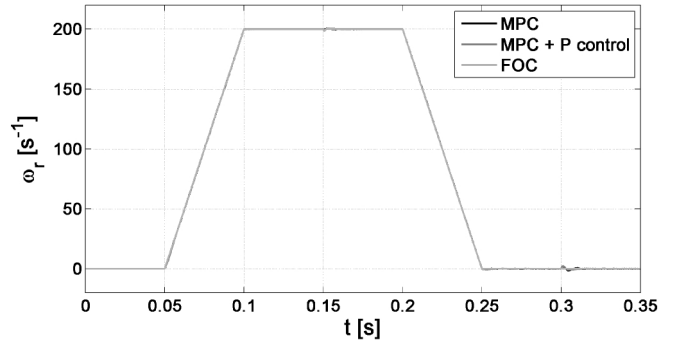


Fig. 5. Simulation comparison of angular speed waveforms.

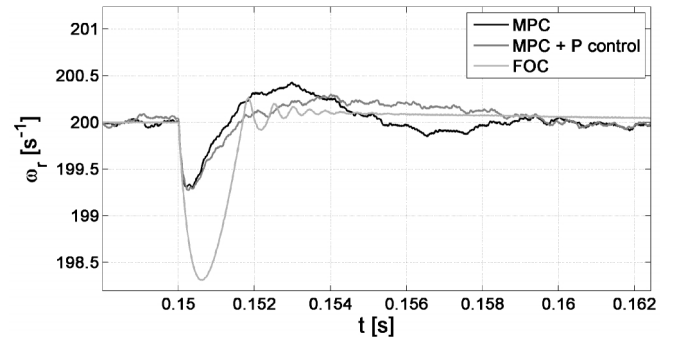


Fig. 6. Speed comparison in detail.

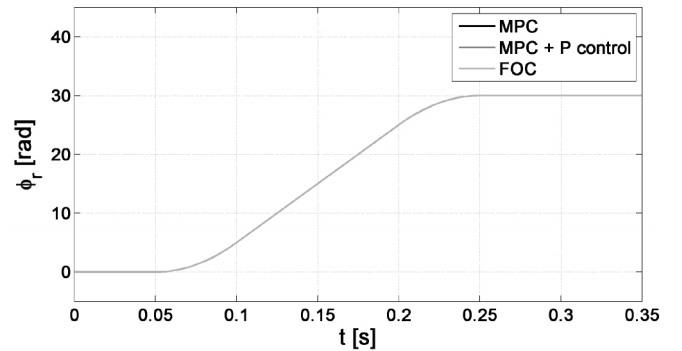


Fig. 7. Position reference tracking.

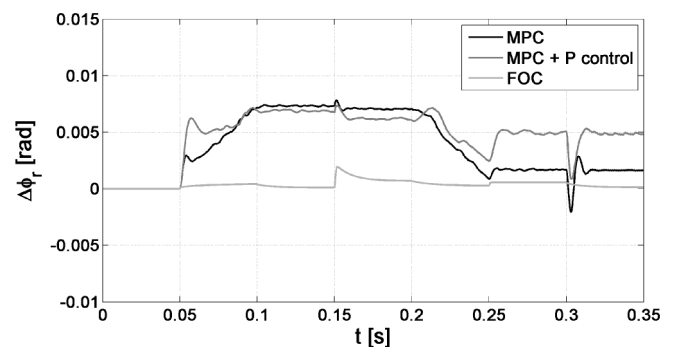


Fig. 8. Position reference following error.

Positioning responses are in Fig. 6 and the position control deviation is depicted in Fig. 7. Here, the FOC structure brings the best results, although the FCS-MPC has satisfactory performance.

VI. CONCLUSIONS

Two different novel structures of the position controllers for PMSM, based on the FCS-MPC, have been presented in this paper. The novelty has been demonstrated in review of the literature. In addition, a new unique cost function has been developed for these controllers. By introducing the feedforward acceleration term and the feedforward load torque term to the cost function, we have shown that the use of such cost function improves the speed and the current control capabilities. The oscillations in current waveforms were minimized and very fast responses to load torque changes were achieved. Even better results can be achieved by using the shorter sampling times, but this is limited by the hardware computing power.

However, the combination of FCS-MPC and proportional controller brings computing time savings without the significant performance decrease comparing to the pure FCS-MPC position controller. The simulation comparison has proven that both presented FCS-MPC approaches are comparable to the FOC control structure in the position accuracy and overcome the FOC dynamics in the speed control.

Considering given facts, FCS-MPC based position control seems to be a promising way to the control of high dynamic electrical drives.

APPENDIX A

TABLE A-I. MOTOR PARAMETERS.

Parameter	Value	Unit
Terminal Resistance	0.12	Ω
Terminal Inductance	0.33	mH
Torque Constant	0.07	Nm.A-1
Pole Pairs	5	-
Rated Current	13	A
Rated Speed	3000	rpm
Motor Inertia	0.000588	kg.m ²

REFERENCES

- [1] F. Genduso, R. Miceli, C. Rando, G. R. Galluzzo, "Back EMF sensorless-control algorithm for high-dynamic performance PMSM", *IEEE Trans. Industrial Electronics*, vol. 57, no. 6, pp. 2092–2100, 2010. [Online]. Available: <http://dx.doi.org/10.1109/TIE.2009.2034182>
- [2] V. Delli Colli, R. Di Stefano, F. Marignetti, "A system-on-chip sensorless control for a permanent-magnet synchronous motor", *IEEE Trans. Industrial Electronics*, vol. 57, no. 11, pp. 3822–3829, 2010. [Online]. Available: <http://dx.doi.org/10.1109/TIE.2009.2039459>
- [3] G. Foo, M. F. Rahman, "Sensorless vector control of interior permanent magnet synchronous motor drives at very low speed without signal injection", *Electric Power Applications, IET*, vol. 4, no. 3, pp. 131–139, 2010. [Online]. Available: <http://dx.doi.org/10.1049/iet-epa.2009.0024>
- [4] Zhaowei Qiao, Tingna Shi, Yindong Wang, Yan Yan, Changliang Xia, Xiangning He, "New sliding-mode observer for position sensorless control of permanent-magnet synchronous motor", *IEEE Trans. Industrial Electronics*, vol. 60, no. 2, pp. 710–719, 2013. [Online]. Available: <https://doi.org/10.1109/TIE.2012.2206359>
- [5] L. Zhong, M. F. Rahman, W. Y. Hu, K. W. Lim, M. A. Rahman, "A direct torque controller for permanent magnet synchronous motor drives", *IEEE Trans. Energy Conversion*, vol. 14, no. 3, pp. 637–642, 1999. [Online]. Available: <http://dx.doi.org/10.1109/60.790928>
- [6] J.-F. Stumper, A. Dotlinger, R. Kennel, "Classical model predictive control of a permanent magnet synchronous motor", *European Power Electronics and Drives Journal*, vol. 22, no. 3, pp. 24–31, 2012. [Online]. Available: <https://doi.org/10.1080/09398368.2012.11463828>
- [7] Shan Chai, Liuping Wang, E. Rogers, "Model predictive control of a permanent magnet synchronous motor", *37th Annual Conf. IEEE Industrial Electronics Society (IECON 2011)*, 2011, pp. 1928–1933, pp. 7–10. [Online]. Available: <https://doi.org/10.1109/iecon.2011.6119601>
- [8] J. Rodriguez, J. Pontt, C. A. Silva, P. Correa, P. Lezana, P. Cortes, U. Ammann, "Predictive current control of a voltage source inverter", *IEEE Trans. Industrial Electronics*, vol. 54, no. 1, pp. 495–503, 2007. [Online]. Available: <http://dx.doi.org/10.1109/TIE.2006.888802>
- [9] M. Pastor, J. Dudrik, M. Vacek, "Predictive power control of grid-tied multilevel inverter", *Acta Electrotechnica et Informatica*, vol. 13, no. 3, pp. 3–7, 2013.
- [10] M. Pastor, J. Dudrik, "Predictive current control of grid-tied cascade h-bridge inverter", *Automatika: Journal for Control, Measurement, Electronics, Computing and Communications*, vol. 54, no. 3, pp. 308–315, 2013.
- [11] F. Morel, Xuefang Lin-Shi, J.-M. Retif, B. Allard, C. Buttay, "A comparative study of predictive current control schemes for a permanent-magnet synchronous machine drive", *IEEE Trans. Industrial Electronics*, vol. 56, no. 7, 2009. [Online]. Available: <https://doi.org/10.1109/TIE.2009.2018429>
- [12] Qian Liu, K. Hmeyer, "A finite control set model predictive direct torque control for the PMSM with MTPA operation and torque ripple minimization", *IEEE Int. Electric Machines and Drives Conf. (IEMDC)*, 2015. [Online]. Available: <https://doi.org/10.1109/iemdc.2015.7409152>
- [13] E. J. Fuentes, J. Rodriguez, C. Silva, S. Diaz, D. E. Quevedo, "Speed control of a permanent magnet synchronous motor using predictive current control", in *IEEE 6th Int. Power Electronics and Motion Control Conf., (IPEMC 2009)*, 2009, pp. 390–395. [Online]. Available: <http://dx.doi.org/10.1109/IPEMC.2009.5157418>
- [14] M. Preindl, S. Bolognani, "Model predictive direct speed control with finite control set of PMSM drive systems", *IEEE Trans. Power Electron.*, vol. 28, no. 2, pp. 1007–1015, 2013. [Online]. Available: <http://dx.doi.org/10.1109/TPEL.2012.2204277>
- [15] E. J. Fuentes, C. A. Silva, J. I. Yuz, "Predictive speed control of a two-mass system driven by a permanent magnet synchronous motor", in *IEEE Trans. Industrial Electronics*, vol. 59, no. 7, pp. 2840–2848, 2012. [Online]. Available: <http://dx.doi.org/10.1109/TIE.2011.2158767>
- [16] P. Pillay, R. Krishnan, "Modelling of permanent magnet motor drives", *IEEE Trans. Industrial Electronics*, vol. 35, no. 4, pp. 357–541, 1988. [Online]. Available: <http://dx.doi.org/10.1109/41.9176>
- [17] V. Slapak, K. Kyslan, F. Mejdr, F. Durovsky, "Determinantion of initial commutation angle offset of permanent magnet synchronous machine – an overview and simulation", *Acta Electrotechnica et Informatica*, vol. 14, no. 4, pp.17–22, 2014. [Online]. Available: <http://dx.doi.org/10.15546/acei-2014-0035>
- [18] C. A. Silva, J. I. Yuz, "On sampled-data models for model predictive control", in *Proc. 36th Annu. IEEE (IECON)*, 2010, pp. 2966–2971, pp. 7–10. [Online]. Available: <http://dx.doi.org/10.1109/IECON.2010.5674939>
- [19] F. Haugen, Kompendium for Kyb. 2 ved Høgskolen i Oslo, Telemark University College, Department of Electrical Engineering, Information Technology and Cybernetics, 2015. [Online]. Available: <http://home.hit.no/~hansha/documents/control/theory/kalmanfilter.pdf>